JACS
JOURNAL OF THE AMERICAN CHEMICAL SOCIETY
Article
pubs.acs.org/JACS

Tunable Charge-Transport Properties of I_h-C_{80} Endohedral Metallofullerenes: Investigation of $La_2@C_{80}$, $Sc_3N@C_{80}$, and $Sc_3C_2@C_{80}$

Satoru Sato,[†] Shu Seki,*[,‡] Guangfu Luo,[§] Mitsuaki Suzuki,[†] Jing Lu,*[,∥] Shigeru Nagase,*[,§] and Takeshi Akasaka*[,†]

[†]Life Science Center of Tsukuba Advanced Research Alliance, University of Tsukuba, Tsukuba, Ibaraki 305-8577, Japan
[‡]Department of Applied Chemistry, Graduate School of Engineering, Osaka University, Suita, Osaka 565-0871, Japan
[§]Fukui Center for Fundamental Chemistry, Kyoto University, Kyoto 606-8103, Japan
[∥]State Key Laboratory of Mesoscopic Physics and Department of Physics, Peking University, Beijing 100871, People's Republic of China

Supporting Information

ABSTRACT: Fullerene crystals or films have drawn much interest because they are good candidates for use in the construction of electronic devices. The results of theoretical calculations revealed that the conductivity properties of I_h-C_{80} endohedral metallofullerenes (EMFs) vary depending on the encapsulated metal species. We experimentally investigated the solid-state structures and charge-carrier mobilities of I_h-C_{80} EMFs $La_2@C_{80}$, $Sc_3N@C_{80}$, and $Sc_3C_2@C_{80}$. The thin film of $Sc_3C_2@C_{80}$ exhibits a high electron mobility μ = 0.13 cm^2 V^{-1} s^{-1} under normal temperature and atmospheric pressure, as determined using flash-photolysis time-resolved microwave conductivity measurements. This electron mobility is 2 orders of magnitude higher than the mobility of $La_2@C_{80}$ or $Sc_3N@C_{80}$.

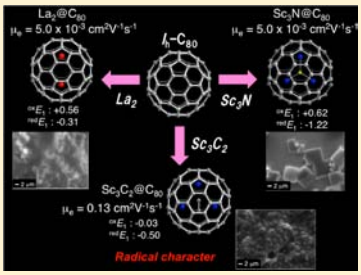

INTRODUCTION

Since the first discovery of C_{60} in 1985,[1] much attention has been devoted to study the solid-state properties of fullerenes and their derivatives because they are a well-known class of n-type semiconductors that are promising candidates for practical application in molecular electronics such as organic thin-film transistors and organic photovoltaic devices.[2] Encapsulation of metal inside fullerene leads to endohedral metallofullerenes (EMFs). Because of the influence of interaction between endohedral metal atoms and the fullerene cage, the electronic properties of EMFs are changed drastically from those of empty fullerenes.[3] For example, $La@C_{82}$ and $La_2@C_{80}$, which are two typical EMFs, respectively have 0.70 and 0.81 V lower first reduction potentials than C_{60}.[4] These facts spurred our interest in investigations of the electronic properties, charge-transport properties, and practical applications of EMFs. One of the important properties of semiconductors is the charge-carrier mobility (μ), which characterizes the charge-transport ability, and a high μ can lead to a high device speed. Early works reported rather low carrier mobilities in monometallofullerenes $M@C_{82}$ (M = Ce, Pr, and Dy)[5] and dimetallofullerene $La_2@C_{80}$.[6] Recently we found that monometallofullerene $La@C_{82}$ has a carrier mobility of >10 cm^2 V^{-1} S^{-1}, which is the highest among organic conductors measured by time-resolved microwave conductivity (TRMC).[7] To the best of our knowledge, the carrier mobilities of dimetallofullerenes and trimetallofullerenes remain open.

Dimetallofullerene $La_2@C_{80}$ (**1**)[8] and trimetallofullerenes $Sc_3N@C_{80}$ (**2**)[9] and $Sc_3C_2@C_{80}$ (**3**)[10] are important because their yields are fairly high and they have the same I_h symmetry as that of the well-known C_{60} molecule, in which high symmetry plays a significant role in various interesting properties. For **1** and **2**, six valence electrons are known to be transferred from endohedral spaces to the C_{80} carbon cage, providing closed-shell electronic structures formally described respectively as $(La^{3+})_2@C_{80}^{6-}$[8c] and $(Sc_3N)^{6+}@C_{80}^{6-}$.[11] Meanwhile, **3** has unique electronic properties such as paramagnetic character.[10] The difference in endohedral species can also induce a change of their electronic properties. For example, the first reduction potentials of **1**, **2**, and **3** are, respectively, −0.31 V,[4b] −1.22 V,[12] and −0.50 V.[10] In this paper we present the charge-carrier mobilities of thin films of **1**−**3** deposited on the substrate using TRMC measurements.[13] TRMC measurements enable electrodeless measurements to be conducted for determination of the intrinsic charge-carrier mobility. The thin film of $Sc_3C_2@C_{80}$ exhibits a high electron mobility μ = 0.13 cm^2 V^{-1} s^{-1} under normal temperature and atmospheric pressure, which is 2 orders of magnitude higher than the mobility of $La_2@C_{80}$ or $Sc_3N@C_{80}$. A first-principles calculation is carried out to analyze the experimental results.

EXPERIMENTAL SECTION

General Procedures. To study the charge-carrier mobilities of thin films, CS_2 solutions of **1**−**3** (about 0.2 mg/mL concentration) were drop-casted onto the quartz substrate. Scanning electron microscopy (SEM; JSM-7001, JEOL Ltd.) observations were conducted at 15.0 kV. Atomic force microscopy (AFM) observations were conducted using a scanning probe microscope (Nano-Navi II,

Received: April 17, 2012
Published: June 18, 2012

dx.doi.org/10.1021/ja303660g | J. Am. Chem. Soc. 2012, 134, 11681−11686

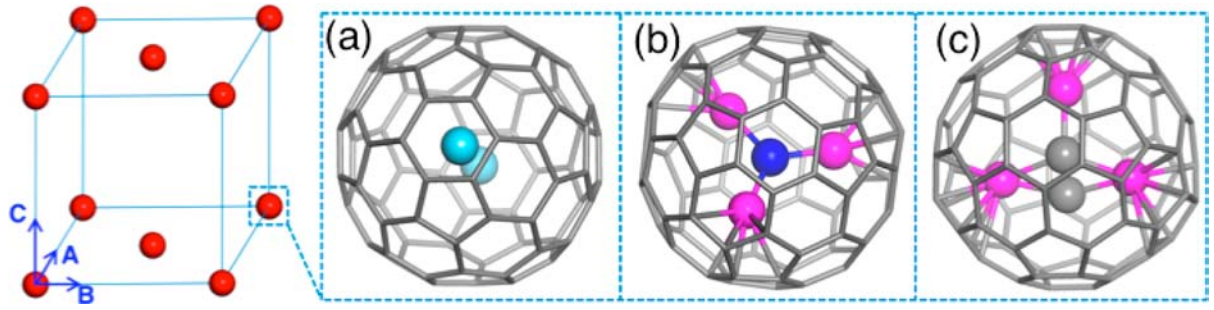

Figure 1. (Left) Schematic structure of the base-centered monoclinic lattice. (Right) Geometrical structures of (a) $La_2@C_{80}$, (b) $Sc_3N@C_{80}$, and (c) $Sc_3C_2@C_{80}$ in the respective optimized crystals.

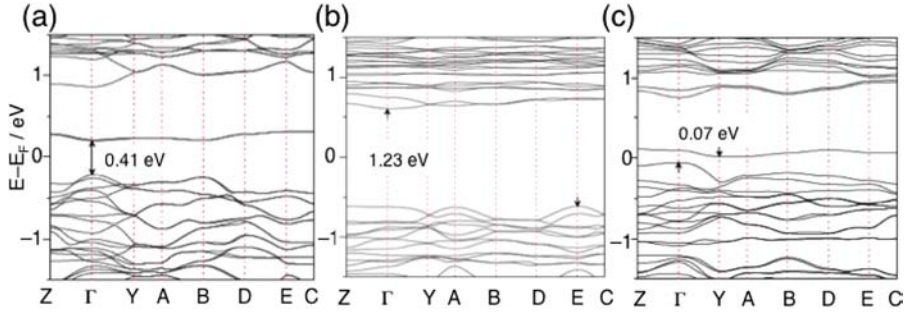

Figure 2. Band structures of the (a) $La_2@C_{80}$, (b) $Sc_3N@C_{80}$, and (c) $Sc_3C_2@C_{80}$ crystals. The corresponding band gap is labeled in each panel.

SII-Nanotechnology Inc.). X-ray diffraction (XRD) patterns were taken (XPert Pro MPD, PANalytical B.V.) with Cu Kα radiation (λ = 1.542 Å) at 45 kV and 40 mA.

Models and Theoretical Methods. On the basis of the experimentally obtained results of $La_2@C_{80}$[8b] (monoclinic lattice, a = 18.2872 Å, b = 11.2120 Å, c = 11.1748 Å, $\alpha = \gamma = 90°$, β = 107.91°) and the nearly 8.5 Å diameter of C_{80}, we deduce that the crystal actually possesses the base-centered monoclinic lattice as shown in Figure 1.[14] In our calculations, we directly adopt the previously described experimental unit cell values. All calculations are conducted using density functional theory (DFT) as implemented in the DMol^3 code.[15] The generalized gradient approximation with the revised Perdew–Burke–Ernzerhof (RPBE) form is used for the exchange-correlation functional. Effective core potentials, which introduce some degree of relativistic correction into the core, are used for Sc and La atoms, although all electrons are considered for C and N atoms. A double numerical plus polarization (DNP) basis set, comparable to the 6-31G basis set, is used. The Brillouin zone is sampled with a k-point spacing of ca. 0.05 Å^{-1}. Atom positions are optimized until the maximum force on each atom is less than 0.027 eV/Å. To consider the possible magnetic properties, spin-polarized effects are considered.

Time-Resolved Microwave Conductivity Measurement. Nanosecond laser pulses from a Nd:YAG laser (second harmonic generation (SHG; 532 nm) and third harmonic generation (THG; 355 nm) from Spectra Physics INDY-HG (fwhm 5–8 ns)) were used as excitation sources. The power density of the laser was set to 0.1–30 mJ/cm^2 ((0.09–5.1) × 10^{16} photons/cm^2). For TRMC measurements, the microwave frequency and power were set respectively to ca. 9.1 GHz and 3 mW, so that the motion of charge carriers cannot be disturbed by the low electric field of the microwave. The TRMC signal picked up by a diode (rise time <1 ns) is monitored using a digital oscilloscope. All experiments described above were conducted at room temperature. The transient photoconductivity ($\Delta\sigma$) of the samples is related to the reflected microwave power ($\Delta P_r/P_r$) and sum of the mobilities of charge carriers via

$$\left\langle \Delta\sigma \right\rangle = \frac{1}{A}\frac{\Delta P_r}{P_r} \quad (1)$$

$$\Delta\sigma = eN\phi \sum \mu \quad (2)$$

where A, e, ϕ, N, and $\sum\mu$ respectively stand for a sensitivity factor, the elementary charge of an electron, the photocarrier generation yield (quantum efficiency), the number of absorbed photons per unit volume, and the sum of mobilities for negative and positive carriers.[16] Polarization of the laser pulses is isotropic. All crystals are mounted on quartz rods and overcoated with polysiloxane. The experimental setup is presented in Figure S1 (Supporting Information). The number of photons absorbed by the crystals is estimated through the direct measurement of transmitted power of laser pulses through a quartz rod–crystal with PMMA binder–quartz rod geometry laser power meter (see Figure S1, NOVA-display; Opher). The quartz rod is rotated in the microwave cavity, and the changes in the effective electric field in the crystals by the rotation of the samples were calibrated on the basis of the geometry of the crystals captured by a digital charge-coupled device (CCD) camera.

The values of ϕ in the compounds were determined using conventional photocurrent measurements in a vacuum chamber (<10^{-5} Pa) with interdigitated Au electrodes and a 5 μm gap under excitation at 355 or 532 nm with a power density of (4.2–5.4) × 10^{16} photons/cm^2. The transient current was observed predominantly under the applied bias of 0–20 V (ca. 0 to 4.0 × 10^4 V cm^{-1}) and monitored using a source meter (2612, Keithley Instruments Inc.). The photocarrier generation yield was estimated using the I–V traces under dark/355 (532) nm illumination conditions. Other details of the apparatus set are described elsewhere.[13]

RESULTS AND DISCUSSION

To provide theoretical insight related to the transport properties of thin films of I_h-C_{80} EMFs, density functional calculations were performed. The optimized geometries are shown in Figure 1, and it was clarified that **1** and **2** are nonmagnetic whereas the two **3** cages have antiferromagnetic interactions in a unit cell. The band structures displayed in Figure 2 show that all three structures are semiconductors with band gaps of 0.41, 1.23, and 0.07, respectively, for **1**–**3**. Such a difference mainly derives from different positions of the

dx.doi.org/10.1021/ja303660g | J. Am. Chem. Soc. 2012, 134, 11681–11686

conduction band minimum (CBM): the CBM resides close to the valence band maximum (VBM) in **1** and **3**, but far from the VBM in **2**. To examine this point further, we show the molecular orbitals of the VBM and CBM at the Γ point in Figure 3. The results show that the molecular orbitals of the

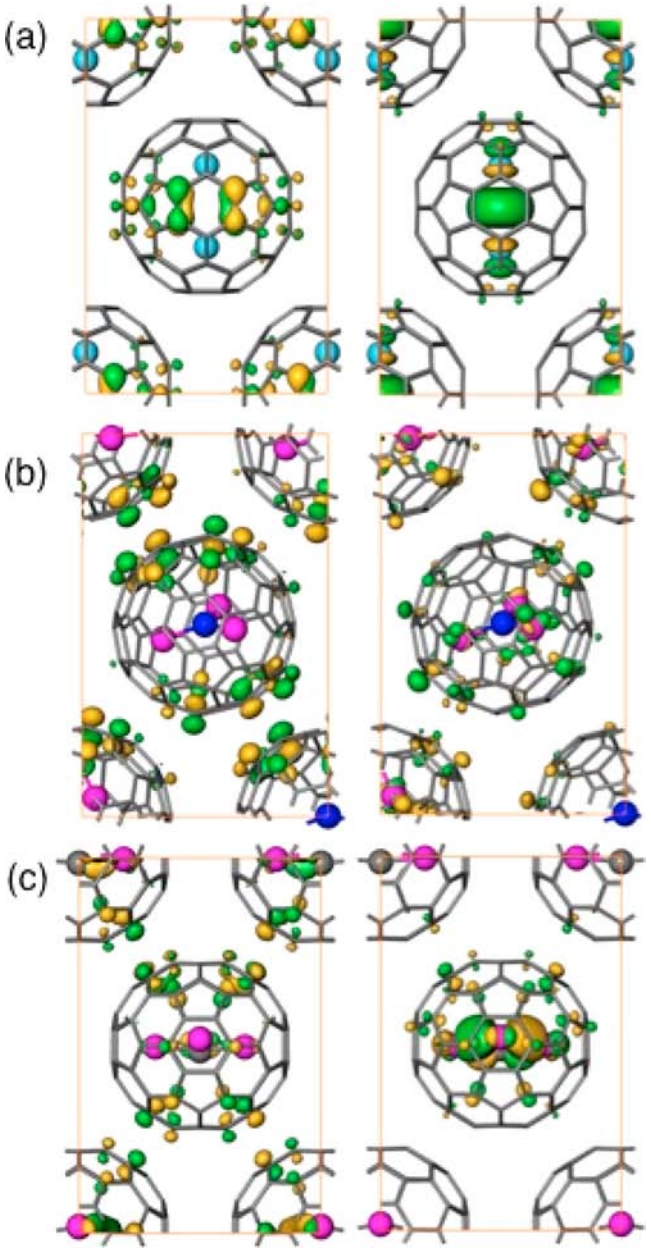

Figure 3. Molecular orbitals of the VBM (left column) and CBM (right column) at the Γ point in the (a) $La_2@C_{80}$, (b) $Sc_3N@C_{80}$, and (c) $Sc_3C_2@C_{80}$ crystals. The isovalue is 0.03 au.

VBM are contributed mainly by I_h-C_{80} for all three systems. However, the molecular orbitals of the CBM have different origins: in **1** and **3**, the orbitals originate mainly from the inner atoms, but in **2**, the orbitals originate mainly from I_h-C_{80} and the inner atoms have little electron density. Therefore, the properties of the inner atoms can strongly affect the crystal band structure.

To investigate the electrical conductivity, the calculated effective masses of the carriers near the Fermi level are provided in Table 1. One can find that the effective masses of the three

Table 1. Band Gap and Effective Mass of the Conduction Band Maximum (m_e*) and Valence Band Minimum (m_h*) of the $La_2@C_{80}$, $Sc_3N@C_{80}$, and $Sc_3C_2@C_{80}$ Crystals[a]

	E_g (eV)	m_e* (m_0)	m_h* (m_0)
$La_2@C_{80}$ (**1**)	0.41	3.7 (Z → Γ)	−1.4 (Z → Γ)
		8.0 (Y → Γ)	−1.5 (Y → Γ)
$Sc_3N@C_{80}$ (**2**)	1.23	4.7 (Z → Γ)	−2.0 (D → E)
		23.0 (Y → Γ)	−1.7 (C → E)
$Sc_3C_2@C_{80}$ (**3**)	0.07	4.5 (Γ → Y)	−14.0 (Z → Γ)
		42.0 (A → Y)	−2.5 (Y → Γ)

[a] m_0 is the mass of a free electron.

structures are generally at the same level: the values of an electron (m_e*) are around $4m_0$ and those of a hole (m_h*) around $-2m_0$. Therefore, the carrier mobility (μ) differences of the three structures are dominated by the collision time (τ) according to $\mu = e\tau/m^*$. For the conductivity (σ), because the band gap (E_g) of **3** is about 1/6 and 1/17 of those of **1** and **2**, respectively, the intrinsic carrier concentration (n) of **3** is over 10^3 times higher than those of the two other structures at room temperature (T = 300 K) according to the formula[17]

$$\sigma = ne(\mu_e + \mu_h) = 2\left(\frac{k_B T}{2\pi\hbar^2}\right)^{3/2} (m_e^* m_h^*)^{3/4} e^{-E_g/2k_B T} e(\mu_e + \mu_h)$$

Thus, **3** probably has much larger conductivity than the other two structures.

To evaluate the charge-carrier mobility experimentally, I_h-C_{80} metallofullerenes **1**−**3** were cast onto the quartz plate. The thin film morphologies for **1**−**3** were characterized using XRD, SEM, and AFM measurements. The XRD measurement displayed some sharp reflections, suggesting that these samples had crystalline features (Figure S2, Supporting Information). The SEM micrographs of the thin films of **1**−**3** obtained from CS_2 solutions are presented in Figure 4. Polycrystalline features are observed in the SEM micrograph of **2**, which contrast against the partially amorphous characteristics of the thin films of **1** and **3**. This point is confirmed by topographic/phase images in AFM measurements of **1**−**3** shown in Figure S3 (Supporting Information). These results show that **2** has higher crystallinity in the solid state than **1** and **3**. This phenomenon was surprising to us because the difference in the solubilities for **1**−**3** in various organic solvents is not so large.

To evaluate the intrinsic charge-carrier mobility (μ) of casted thin films of **1**−**3**, TRMC measurements were performed on the deposited thin films of **1**−**3**. Upon exposure to a laser pulse with an excitation wavelength of 355 nm, all samples revealed transient conductivity $\langle\phi\sum\mu\rangle$, where ϕ and $\sum\mu$ respectively denote the photocarrier generation yield (quantum efficiency) and the sum of mobilities for positive and negative charge carriers. The ϕ values were determined using conventional dc-current integration with semitransparent Au electrodes as counter electrodes under excitation at 355 nm. It is noteworthy that, for all films, the current transients are observed in negative bias mode, suggesting that electrons are the major charge-carrier species. The observed values of $\phi\sum\mu$ (Figure 5a), ϕ, and μ are presented in Table 2. The μ value of **3** is the same as that reported for $La@C_{82}$[18] and 2 orders magnitude higher than those of **1** and **2**. Although this value is evaluated in the film state, the observed electron mobility of **3** (0.13 $cm^2\ V^{-1}\ s^{-1}$) is

dx.doi.org/10.1021/ja303660g | J. Am. Chem. Soc. 2012, 134, 11681−11686

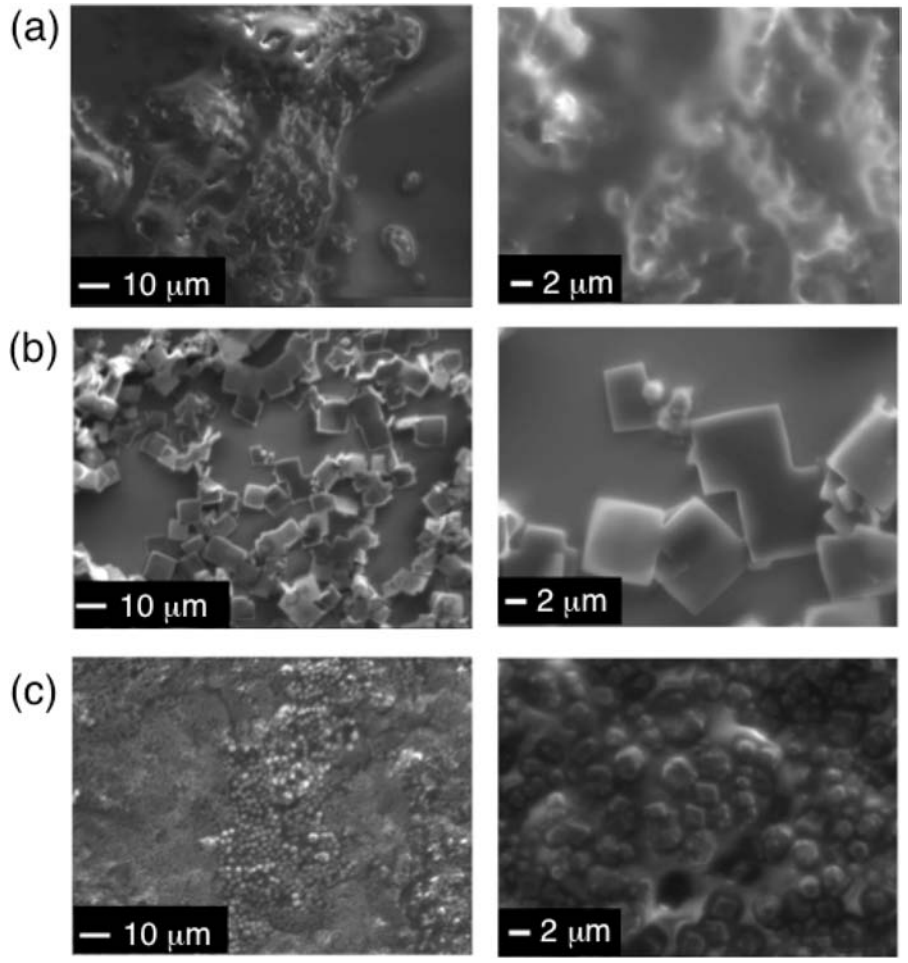

Figure 4. SEM images of the thin films of (a) $La_2@C_{80}$, (b) $Sc_3N@C_{80}$, and (c) $Sc_3C_2@C_{80}$.

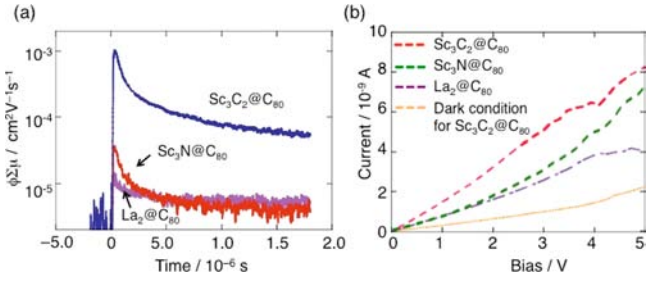

Figure 5. (a) Conductivity transients observed for polycrystalline solvent-casted films of **1**−**3** upon excitation at 355 nm and (1.4−1.9) × 10^{16} photons cm^{-2}. The measurement was carried out under air conditions at room temperature. (b) *I*−*V* characteristics of **1**−**3** casted films on Au interdigitated electrodes with a 5 μm gap. Illumination was carried out at 355 nm and 10.5 mW cm^{-2}. The orange line is the *I*−*V* trace observed under dark conditions for a **3** casted film on the electrode.

fairly close to that of a single crystal of C_{60} (0.5 cm^2 V^{-1} s^{-1} determined by time-of-flight measurement[19]) and considerably high among the n-type materials. The fact that **3** and $La@C_{82}$ showed extremely high electron mobility compared to **1** and **2** might be related to their radical character, which leads to stable anion species generated by photoinduced charge-carrier generation and facilitates the movement of electrons. However, **1** and **2** showed much lower electron mobility than **3** did. In terms of electron affinity, a lower reduction potential engenders the advantage of electron injection and air stability of their anions,[20] suggesting that **1** might show the higher electron transport property. However, orbital delocalization on the I_h-C_{80} cage in CBM (Figure 3b) and high ordering molecular alignment of **2** caused the formation of the path of charge carriers, indicated as high electron mobility of **1**.

Table 2. Electrochemical Properties, Conductivity Transient ($\phi\sum\mu$), Charge-Carrier Generation Yield (ϕ), and Charge-Carrier Mobility (μ) of the Thin Films of $La_2@C_{80}$, $Sc_3N@C_{80}$, $Sc_3C_2@C_{80}$, and $La@C_{82}$

	E_1^{ox} (V[a])	E_1^{red} (V[a])	$\phi\sum\mu$ (cm^2 V^{-1} s^{-1})	ϕ (%)	μ (cm^2 V^{-1} s^{-1})
$La_2@C_{80}$ (**1**)	0.56[b]	−0.31[b]	1.0×10^{-5}	0.2	5.0×10^{-3}
$Sc_3N@C_{80}$ (**2**)	0.62[c]	−1.22[c]	4.0×10^{-5}	0.70	5.7×10^{-3}
$Sc_3C_2@C_{80}$ (**3**)	−0.03[d]	−0.50[d]	1.0×10^{-3}	0.75	0.13
$La@C_{82}$	0.07[e]	−0.42[e]	2.0×10^{-4}[f]	0.15[f]	0.13[f]

[a]Volts vs Fc/Fc^+. [b]Reference 4b. [c]Reference 12. [d]Reference 10. [e]Reference 4a. [f]Reference 18.

Figure 5b shows the *I*−*V* trace measurement of casted thin films of **1**−**3**. One can find that **3** has obviously larger conductivity than **1** and **2**, which confirms our earlier estimation. Furthermore, it is noteworthy that the cast film of **3** exhibits a considerable dark current, which indicates that the thin film of **3** can conduct current without generation of charge

dx.doi.org/10.1021/ja303660g | J. Am. Chem. Soc. 2012, 134, 11681−11686

carriers and the solid state of **3** works as an organic conductor just like the single crystal of the La@C_{82} derivative.[7] The good conductivity of **3** is consistent with our DFT calculations. Physically, at room temperature, the valence electrons of **3** can be easily excited across the very small band gap to the conduction bands, creating sufficient electron and hole carriers in the crystal. Consequently, **3** can be regarded as a semimetal and has high conductivity.

CONCLUSION

In conclusion, we investigated the charge-carrier mobility of thin films of I_h-C_{80} endohedral metallofullerenes **1**−**3** using TRMC measurements. XRD, SEM, and AFM measurements revealed that these three thin films have crystalline structures; especially **2** has polycrystalline features. The observed electron mobility of **3** was much greater than that of **1** or **2**. The paramagnetic property of **3** is expected to be mainly attributable to the presentation of high electron mobility. Theoretical calculations revealed that the effect of endohedral doping is important in modifying the conduction character. Our findings enhance the potential utility of EMF materials for practical applications.

ASSOCIATED CONTENT

Supporting Information

Schematic showing the setup of the TRMC measurement and XRD patterns and AFM images of **1**−**3**. This material is available free of charge via the Internet at http://pubs.acs.org.

AUTHOR INFORMATION

Corresponding Author

akasaka@tara.tsukuba.ac.jp

Notes

The authors declare no competing financial interest.

ACKNOWLEDGMENTS

This work was supported in part by a Grant-in-Aid for Scientific Research in Innovation Areas (20108001, "pi-Space"), a Grant-in-Aid for Scientific Research (A) (20245006), The Next Generation Super Computing Project (Nanoscience Project), the Nanotechnology Support Project, and Grants-in Aid for Scientific Research in Priority Areas (20036008, 20038007) and Specially Promoted Research (22000009) from the Ministry of Education, Culture, Sports, Science, and Technology of Japan. We thank Prof. Toshiharu Teranishi, Kyoto University, for the XRD measurement. S.Sa. thanks the Japan Society for the Promotion of Science for Research Fellowships for Young Scientists. J.L. is supported by the National Natural Science Foundation of China (Grant 10774003) and National 973 Projects (Grant 2007CB936200, Most of China).

REFERENCES

(1) Kroto, H. W.; Heath, J. R.; O'Brien, S. C.; Curl, R. F.; Smalley, R. E. *Nature* **1985**, *318*, 162−163.

(2) (a) Liang, Y.; Yu, L. *Acc. Chem. Res.* **2010**, *43*, 1227−1236. (b) Peet, J.; Heeger, A. J.; Bazan, G. C. *Acc. Chem. Res.* **2009**, *42*, 1700−1708. (c) Martin, N.; Sánchez, L.; Herranz, M. A.; Illescas, B.; Guldi, D. M. *Acc. Chem. Res.* **2007**, *40*, 1015−1024. (d) Mirikin, C. A.; Caldwell, W. B. *Tetrahedron* **1996**, *52*, 5113−5130. (e) Guldi, D. M.; Illescas, B. M.; Atienza, C. M.; Wielopolski, M.; Martin, N. *Chem. Soc. Rev.* **2009**, *38*, 1587−1597. (f) Priebe, G.; Pietzak, B.; Könenkamp, R. *Appl. Phys. Lett.* **1997**, *71*, 2160−2162. (g) Anthopoulos, T. D.; Ramil, A. M.; Sitter, H.; Cölle, M.; Leeuw, D. M. *Appl. Phys. Lett.* **2006**, *89*, 213504. (h) Pinzón, J. R.; Villalta−Cerdas, A.; Echegoyen, L. *Top. Curr. Chem.* **2012**, *312*, 127−174.

(3) (a) *Endofullerenes: A New Family of Carbon Clusters*; Akasaka, T., Nagase, S., Eds.; Kluwer: Dordrecht, The Netherlands, 2002. (b) *Chemistry of Nanocarbons*; Akasaka, T., Wudl, F., Nagase, S., Eds.; Wiley-Blackwell: London, 2010. (c) Chaur, M. N.; Melin, F.; Ortiz, A. L.; Echegoyen, L. *Angew. Chem., Int. Ed.* **2009**, *48*, 7514−7538. (d) Lu, X.; Akasaka, T.; Nagase, S. *Chem. Commun.* **2011**, *47*, 5942−5957. (e) Osuna, S.; Swart, M.; Solà, M. *Phys. Chem. Chem. Phys.* **2011**, *13*, 3585−3603.

(4) (a) Suzuki, T.; Maruyama, Y.; Kato, T.; Kikuchi, K.; Achiba, Y. *J. Am. Chem. Soc.* **1993**, *115*, 11006−11007. (b) Suzuki, T.; Maruyama, Y.; Kato, T.; Kikuchi, K.; Nakao, Y.; Achiba, Y.; Kobayashi, K.; Nagase, S. *Angew. Chem., Int. Ed. Engl.* **1995**, *34*, 1094−1096.

(5) (a) Kanbara, T.; Shibata, K.; Fujiki, S.; Kubozono, Y.; Kashino, S.; Urisu, T.; Sakai, M.; Fujiwara, A.; Kumashiro, R.; Tanigaki, K. *Chem. Phys. Lett.* **2003**, *379*, 223−229. (b) Rikiishi, Y.; Kubozono, Y.; Hosokawa, T.; Shibata, K.; Haruyama, Y.; Takabayashi, Y.; Fujiwara, A.; Kobayashi, S.; Mori, S.; Iwasa, Y. *J. Phys. Chem. B* **2004**, *108*, 7580−7585. (c) Nagano, T.; Kuwahara, E.; Takayanagi, T.; Kubozono, Y.; Fujiwara, A. *Chem. Phys. Lett.* **2005**, *409*, 187−191.

(6) Kobayashi, S.; Mori, S.; Iida, S.; Ando, H.; Takenobu, T.; Taguchi, Y.; Fujiwara, A.; Taninaka, A.; Shinohara, H.; Iwasa, Y. *J. Am. Chem. Soc.* **2003**, *125*, 8116−8117.

(7) Sato, S.; Seki, S.; Honsho, Y.; Wang, L.; Nikawa, H.; Luo, G.; Lu, J.; Haranaka, M.; Tsuchiya, T.; Nagase, S.; Akasaka, T. *J. Am. Chem. Soc.* **2011**, *133*, 2766−2771.

(8) (a) Akasaka, T.; Nagase, S.; Kobayashi, K.; Waelchli, M.; Yamamoto, K.; Funasaka, H.; Kako, M.; Hoshino, T.; Erata, T. *Angew. Chem., Int. Ed. Engl.* **1997**, *36*, 1643−1645. (b) Nishibori, E.; Takata, M.; Sakata, M.; Taninaka, A.; Shinohara, H. *Angew. Chem., Int. Ed.* **2001**, *40*, 2998−2999. (c) Kobayashi, K.; Nagase, S.; Akasaka, T. *Chem. Phys. Lett.* **1995**, *245*, 230−236.

(9) Stevenson, S.; Rice, G.; Glass, T.; Harish, K.; Cromer, F.; Jordan, M. R.; Kraft, J.; Hadji, E.; Bible, R.; Olmstead, M. M.; Maitra, K.; Fisher, A. J.; Balch, A. L.; Dorn, H. C. *Nature* **1999**, *300*, 379−384.

(10) Iiduka, Y.; Wakahara, T.; Nakahodo, T.; Tsuchiya, T.; Sakuraba, A.; Maeda, Y.; Akasaka, T.; Yoza, K.; Horn, E.; Kato, T.; Liu, M. T. H.; Mizorogi, N.; Kobayashi, K.; Nagase, S. *J. Am. Chem. Soc.* **2005**, *127*, 12500−12501.

(11) (a) Campanera, J. M.; Bo, C.; Olmstead, M. M.; Balch, A. L.; Poblet, J. M. *J. Phys. Chem. A* **2002**, *106*, 12356−12364. (b) Kobayashi, K.; Sano, Y.; Nagase, S. *J. Comput. Chem.* **2001**, *13*, 1353−1358.

(12) (a) Krause, M.; Dunsch, L. *ChemPhysChem* **2004**, *5*, 1445−1449. (b) Iiduka, Y.; Ikenaga, O.; Sakuraba, A.; Wakahara, T.; Tsuchiya, T.; Maeda, Y.; Nakahodo, T.; Akasaka, T.; Kako, M.; Mizorogi, N.; Nagase, S. *J. Am. Chem. Soc.* **2005**, *127*, 9956−9957.

(13) (a) Amaya, T.; Seki, S.; Moriuchi, T.; Nakamoto, K.; Nakata, T.; Sakane, H.; Saeki, A.; Tagawa, S.; Hirao, T. *J. Am. Chem. Soc.* **2009**, *131*, 408−409. (b) Seki, S.; Yoshida, Y.; Tagawa, S.; Asai, K.; Ishigure, K.; Furukawa, K.; Fujiki, M.; Matsumoto, N. *Philos. Mag. B* **1999**, *79*, 1631−1645. (c) Imahori, H.; Ueda, M.; Kang, S.; Hayashi, H.; Hayashi, S.; Kaji, H.; Seki, S.; Saeki, A.; Tagawa, S.; Umeyama, T.; Matano, Y.; Yoshida, K.; Isoda, S.; Shiro, M.; Tkachenko, N. V.; Lemmetyinen, H. *Chem.—Eur. J.* **2007**, *13*, 10182−10193. (d) Hisaki, I.; Sakamoto, Y.; Shigemitsu, H.; Tohnai, N.; Miyata, M.; Seki, S.; Saeki, A.; Tagawa, S. *Chem.—Eur. J.* **2008**, *14*, 4178−4187. (e) Saeki, A.; Seki, S.; Takenobu, T.; Iwasa, Y.; Tagawa, S. *Adv. Mater.* **2008**, *20*, 920−923.

(14) Two types of monoclinic lattices exist: one is the simple monoclinic (sm) lattice, and the other is the base-centered monoclinic (bcm) lattice, whose unit cells respectively contain one and two atoms/clusters. Because the nearest distance between neighbor cages in the sm lattice is close to 10 Å in the *a* direction, the crystal can only be the bcm lattice.

(15) (a) Delley, B. *J. Chem. Phys.* **1990**, *92*, 508−517. (b) Delley, B. *J. Chem. Phys.* **2000**, *113*, 7756−7764.

(16) (a) Grozema, F. C.; Siebbeles, L. D. A.; Warman, J. M.; Seki, S.; Tagawa, S.; Scherf, U. *Adv. Mater.* **2002**, *14*, 228−231. (b) Acharya, A.;

Seki, S.; Saeki, A.; Koizumi, Y.; Tagawa, S. *Chem. Phys. Lett.* **2005**, *404*, 356−360. (c) Saeki, A.; Seki, S.; Sunagawa, T.; Ushida, K.; Tagawa, S. *Philos. Mag.* **2006**, *86*, 1261−1276. (d) Nagashima, K.; Yanagida, T.; Tanaka, H.; Seki, S.; Saeki, A.; Tagawa, S.; Kawai, T. *J. Am. Chem. Soc.* **2008**, *130*, 5378−5382.

(17) *Introduction to Solid States Physics*, 8th ed.; Kittel, C., Eds.; John Wiley and Sons: Hoboken, NJ, 2005; p 208.

(18) Sato, S.; Nikawa, H.; Seki, S.; Wang, L.; Luo, G.; Lu, J.; Haranaka, M.; Tsuchiya, T.; Nagase, S.; Akasaka, T. *Angew. Chem., Int. Ed.* **2012**, *51*, 1589−1591.

(19) Frankevich, E.; Maruyama, Y.; Ogata, H. *Chem. Phys. Lett.* **1993**, *214*, 39−44.

(20) (a) Wang, C.; Dong, H.; Hu, W.; Liu, Y.; Zhu, D. *Chem. Rev.* **2012**, *112*, 2208−2267. (b) Babel, A.; Jenekhe, S. A. *J. Am. Chem. Soc.* **2003**, *125*, 13656−13657. (c) Dimitrakopoulos, C. D.; Malenfant, P. R. L. *Adv. Mater.* **2002**, *14*, 99−117. (d) Horowitz, G. *Adv. Mater.* **1998**, *10*, 365−377.